Journal of Magnetic Resonance 205 (2010) 125–129

Contents lists available at ScienceDirect

Journal of Magnetic Resonance

journal homepage: www.elsevier.com/locate/jmr

A selective ^{15}N-to-^{1}H polarization transfer sequence for more sensitive detection of ^{15}N-choline

Jessica A. Pfeilsticker, Jason E. Ollerenshaw, Valerie A. Norton, Daniel P. Weitekamp *

A.A. Noyes Laboratory of Chemical Physics, California Institute of Technology, Pasadena, CA 91125, USA

ARTICLE INFO

Article history:
Received 28 July 2009
Revised 17 March 2010
Available online 27 April 2010

Keywords:
INEPT
PASADENA
^{15}N-choline
Hyperpolarization
Selective coherence transfer
REBURP

ABSTRACT

The sensitivity and information content of heteronuclear nuclear magnetic resonance is frequently optimized by transferring spin order of spectroscopic interest to the isotope of highest detection sensitivity prior to observation. This strategy is extended to ^{15}N-choline using the scalar couplings to transfer polarization from ^{15}N to choline's nine methyl ^{1}H spins in high field. A theoretical analysis of a sequence using nonselective pulses shows that the optimal efficiency of this transfer is decreased by 62% as the result of competing ^{15}N–^{1}H couplings involving choline's four methylene protons. We have therefore incorporated a frequency-selective pulse to support evolution of only the ^{15}N–methyl ^{1}H coupling during the transfer period. This sequence provides a 52% sensitivity enhancement over the nonselective version in *in vitro* experiments on a sample of thermally polarized ^{15}N-choline in D_2O. Further, the ^{15}N T_1 of choline in D_2O was measured to be 217 ± 38 s, the ^{15}N–methyl ^{1}H coupling constant was found to be 0.817 ± 0.001 Hz, and the larger of choline's two ^{15}N–methylene ^{1}H coupling constants was found to be 3.64 ± 0.01 Hz. Possible improvements and applications to *in vivo* experiments using long-lived hyperpolarized heteronuclear spin order are discussed.

1. Introduction

It is now possible to routinely generate samples of certain small biomolecules with nuclear polarizations on the order of 10% using parahydrogen and synthesis allow dramatically enhanced nuclear alignment (PASADENA) [1] or dynamic nuclear polarization (DNP) [2,3]. These technologies show promise for clinical applications based on the *in vivo* characterization of metabolic processes on the seconds timescale. Experiments of this nature rely on storage of the polarization on heteronuclei with long population relaxation times, such as carbonyl ^{13}C or quaternary ^{15}N nuclei, in order to minimize relaxation losses during sample delivery and to provide time for transport, binding, and metabolism. However, the sensitivity enhancement afforded by this strategy is partly lost if the final signal is also detected on a low-γ heteronucleus. Chekmenev et al. [4] have proposed that optimal sensitivity can be obtained by storing polarization on a slowly-relaxing heteronuclear spin and then using an INEPT [5] sequence to coherently transfer magnetization to nearby ^{1}H nuclei for detection, and have demonstrated the method with two hyperpolarized reagents, 1-^{13}C-succinate-d_2 and 2,2,3,3-tetrafluoropropyl 1-^{13}C-propionate-d_3 (TFPP). Those experiments were designed numerically assuming that the relevant ^{1}H and ^{13}C sites were 3-spin ABX systems. A similar strategy has been applied to ^{15}N-choline, where the hyperpolarized ^{15}N polarization was transferred by nonselective INEPT resulting in detectable signal on some of the proton sites [6].

Here we demonstrate a selective version of this polarization transfer strategy with ^{15}N-choline, an $A_9BB'CC'X$ system of 14 spin 1/2 nuclei [7]. Choline is a useful biomarker, showing significantly altered uptake and metabolism in diseased brain tissue [8] and in malignant tumor cells in the breast and prostate [9,10], though toxicity may limit the dose in some applications. Hyperpolarization of ^{15}N-choline to (4.6 ± 1)% has been reported after 2 h of DNP at 1.4 K [3,6]. The ^{15}N longitudinal relaxation time of T_1 = 120 s in blood [3] is promising for metabolic studies.

We have investigated two INEPT-based pulse sequences for ^{15}N-to-^{1}H polarization transfer in ^{15}N-choline. The first is a nonselective refocused INEPT sequence similar to that used in recent hyperpolarized experiments [4,6]. While this sequence is effective, a product operator analysis shows that significantly greater sensitivity can be obtained by using a selective sequence, as demonstrated by targeting choline's nine degenerate methyl ^{1}H spins. We therefore also present a selective refocused INEPT transfer that uses a REBURP pulse to support coherence transfer from ^{15}N to choline's methyl ^{1}H spins while suppressing competing transfer pathways to methylene ^{1}H nuclei. These pulse sequences are experimentally demonstrated *in vitro* using a thermally polarized sample of ^{15}N-choline in aqueous solution.

* Corresponding author. Fax: +1 626 395 6948.
E-mail address: weitekamp@caltech.edu (D.P. Weitekamp).

1090-7807/$ - see front matter © 2010 Elsevier Inc. All rights reserved.
doi:10.1016/j.jmr.2010.04.010

2. Theory

At a given spin polarization and probe efficiency, the sensitivity of detection in an NMR experiment scales as the square of the gyromagnetic ratio of the nuclide being observed. In the case of ^{15}N hyperpolarization, therefore, a voltage enhancement of $(\gamma_{^1H}/\gamma_{^{15}N})^2 = 97$ can be obtained by transferring to ^{1}H for detection rather than directly observing a ^{15}N signal, assuming unity transfer of spin angular momentum, as is closely approached within an isolated ^{15}N–^{1}H spin pair with a resolved scalar coupling. Such a transfer can be achieved using refocused INEPT (Fig. 1), the standard pulse sequence for polarization transfer between spins sharing a dominant scalar coupling. The effect of this sequence when applied to ^{15}N-choline can be determined using a product operator analysis. In the following discussion the relevant ^{15}N–^{1}H scalar coupling constants will be labeled J_m, J_a, and J_b as indicated in Fig. 2. Couplings between the methyl and methylene ^{1}H spins are relatively unimportant and are neglected to make the calculations tractable.

First, consider the effect of the sequence on the spin system of Fig. 2, while initially neglecting the effects of the ^{15}N–methylene ^{1}H couplings J_a and J_b. The system's magnetization is proportional to the dimensionless ^{15}N spin angular momentum, with initial value normalized to $\rho_0 = S_z$. This is converted to in-phase ^{15}N single-quantum coherence by the first ^{15}N $(\pi/2)_x$ pulse to obtain $\rho_1 = -S_y$. This coherence evolves under the ^{15}N–methyl ^{1}H scalar couplings during the INEPT transfer period τ_1 to produce terms that are antiphase with respect to the methyl ^{1}H spins. The simultaneous π pulses in the middle of τ_1 refocus chemical shift evolution, leaving only the effects of couplings between ^{15}N and each of the nine methyl ^{1}H spins. At the end of τ_1 the system's state is given by

$$\rho_2 = -S_y \cos^9(\pi J_m \tau_1) + \sum_{i=1}^{9} 2S_x I_{iz} \cos^8(\pi J_m \tau_1) \sin(\pi J_m \tau_1) + \sum_{i=1}^{8} \sum_{j=i+1}^{9} 4S_y I_{iz} I_{jz} \cos^7(\pi J_m \tau_1) \sin^2(\pi J_m \tau_1) + HO.$$

Here, *HO* indicates higher-order terms, specifically single-quantum ^{15}N coherence that is antiphase with respect to three or more ^{1}H spins. After the transfer delay, simultaneous ^{1}H $(\pi/2)_x$ and ^{15}N $(\pi/2)_y$ pulses are applied to give

$$\rho_3 = -S_y \cos^9(\pi J_m \tau_1) + \sum_{i=1}^{9} 2S_z I_{iy} \cos^8(\pi J_m \tau_1) \sin(\pi J_m \tau_1) + \sum_{i=1}^{8} \sum_{j=i+1}^{9} 4S_y I_{iy} I_{jy} \cos^7(\pi J_m \tau_1) \sin^2(\pi J_m \tau_1) + HQ.$$

The pulses convert the terms *HO* to high-order multiple-quantum coherences, which have been abbreviated as *HQ*. At this point, ^{15}N coherences and multiple-quantum ^{1}H coherences, which will not lead to observable signals at the end of the experiment, can be dropped from the density operator. This leaves only single-quantum ^{1}H coherences that are antiphase with respect to ^{15}N,

$$\rho_3 = \sum_{i=1}^{9} 2S_z I_{iy} \cos^8(\pi J_m \tau_1) \sin(\pi J_m \tau_1).$$

The next part of the sequence is a refocusing period of duration $\tau_2 = 1/(2J_m)$ during which the antiphase single-quantum ^{1}H terms evolve into in-phase ^{1}H coherence

$$\rho_4 = -\sum_{i=1}^{9} I_{ix} \cos^8(\pi J_m \tau_1) \sin(\pi J_m \tau_1).$$

The detected ^{1}H signal is proportional to the total magnetization of the nine methyl protons, so the dependence of the initial signal amplitude on τ_1 is

$$S_{sel} = A_{sel} 9 \cos^8(\pi J_m \tau_1) \sin(\pi J_m \tau_1) + C. \quad (1)$$

This expression includes a hardware-dependent proportionality constant A_{sel} and a constant C accounting for any DC offset in the observed signal. Eq. (1) is similar to the expression derived by Doddrell et al. for a coherence transfer in the opposite direction, from n equivalent ^{1}H spins to a heteronucleus [11]. The value of τ_1 that maximizes S_{sel} is given by

$$\tau_1 = \frac{1}{\pi J_m} \tan^{-1}\left(\frac{1}{2\sqrt{2}}\right).$$

For the value $J_m = 0.82$ Hz measured experimentally for ^{15}N-choline, the optimal transfer delay is $\tau_1 = 0.132$ s, yielding $S_{sel} = 1.873 A_{sel} + C$. The transfer function of the angular momentum from ^{15}N to ^{1}H (Eq. (1)) or vice versa [11] can exceed unity. The conserved quantity is the sum of the squares of the coefficients of the normalized product operators expressing the density operator. Contributions to the observable signal from choline's nine methyl ^{1}H spins combine linearly and constructively at the optimized value of τ_1.

The above calculation is readily generalized to include the effects of scalar coupling between the ^{15}N spin and the four methylene protons (J_a and J_b in Fig. 2), yielding an analogous relative signal function

$$S_{non} = A_{non} 9 \cos^8(\pi J_m \tau_1) \sin(\pi J_m \tau_1) \cos^2(\pi J_a \tau_1) \cos^2(\pi J_b \tau_1) + C. \quad (2)$$

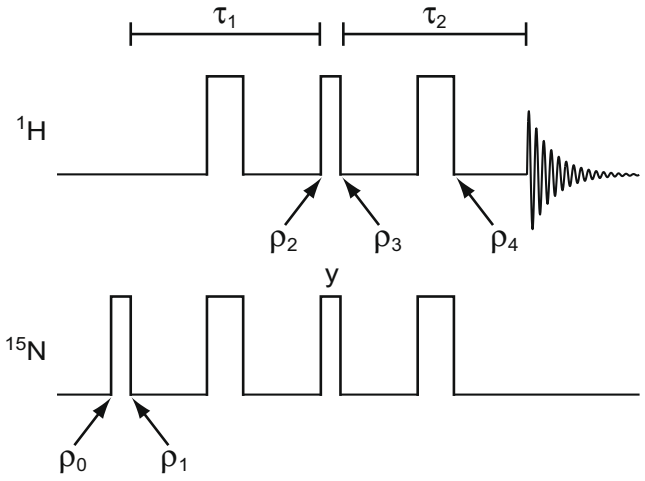

Fig. 1. A refocused INEPT pulse sequence for polarization transfer from ^{15}N to ^{1}H for detection. Narrow (wide) rectangles denote radiofrequency pulses with a tip angle of $\pi/2$ (π). All pulses are applied along the x axis except where indicated.

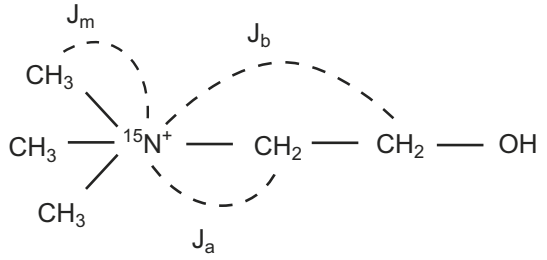

Fig. 2. The structure of ^{15}N-choline. Labels indicate the relevant ^{15}N–^{1}H scalar couplings.

A proportionality constant A_{non} and a DC offset constant C have again been included. Maximizing this function numerically for the best known values of the three coupling constants for choline, $J_m = 0.82$ Hz, $J_a = -0.57$ Hz, $J_b = 3.64$ Hz, gives an optimal transfer delay $\tau_1 = 0.233$ s, which yields a signal of $S_{non} = 0.721A_{non} + C$.

Comparing the maximum values of S_{sel} and S_{non}, it is apparent that the ^{15}N–methylene ^{1}H couplings have the effect of reducing the observable ^{1}H signal by 62% in the idealized case of an experiment for which $A_{sel} = A_{non}$ and $C = 0$. It would clearly be advantageous to suppress these couplings. This can be achieved by replacing the ^{1}H π pulse in the middle of τ_1 with a selective pulse tailored to invert the methyl ^{1}H spins without affecting the methylene ^{1}H spins.

3. Experimental

Data were collected on a Varian ^{UNITY}*INOVA* spectrometer operating at a ^{1}H resonance frequency of 500 MHz. The sample was prepared by dissolving 20 mg ^{15}N-choline chloride (ISOTEC, Miamisburg, Ohio) in 700 µl D_2O. Refocused INEPT experiments were performed using the pulse sequence shown in Fig. 3, which implements the selective ^{15}N–methyl ^{1}H transfer described in the theory section using a 6.695 ms ^{1}H REBURP pulse [12] centered at the methyl ^{1}H frequency. A time $\tau_{reb} = 6.4$ ms, equal to the effective evolution time of the ^{15}N–methyl ^{1}H coupling during the REBURP pulse, was subtracted from the transfer delay as indicated in Fig. 3. For nonselective INEPT experiments, the REBURP was replaced with a nonselective π pulse and τ_{reb} was set to zero.

To allow efficient testing in the absence of hyperpolarization, the sequence includes a ^{15}N purge element before the recycle delay d_1 to ensure that the system reaches a consistent state at the start of each transient. This measure is necessary because it is impractical to allow full relaxation of the choline ^{15}N spin after each transient owing to its very long T_1. The sequence includes a ^{15}N $\pi/2$ pulse immediately prior to acquisition in order to purge any ^{1}H coherence that remains antiphase with respect to ^{15}N after the refocusing period. In the absence of this pulse, intermittent phase aberrations were observed in the methyl ^{1}H resonance.

For ^{15}N T_1 measurements by inversion-recovery, the pulse sequence of Fig. 3 was modified by adding a ^{15}N π pulse and a variable recovery delay immediately before the ^{1}H purge pulse. For these experiments, the ^{15}N purge element before d_1 was removed and d_1 was increased to 600 s.

Data analysis was performed in MATLAB (The MathWorks, Natick, MA) using scripts developed in house. Spectral data were quantified by fitting to a complex Lorentzian lineshape function, except for inversion-recovery data, which was quantified by integration. A downhill simplex algorithm was used for least-squares data fitting, and uncertainties in the extracted parameters were estimated using a bootstrap Monte Carlo method [13].

The value of τ_{reb}, which is subtracted from the INEPT transfer delay in order to account for evolution of the ^{15}N–methyl ^{1}H scalar coupling during the long REBURP pulse, was determined using a numerical simulation of the pulse sequence. Calculations were performed in GAMMA v4.1.2 [14] in Hilbert space using a spin system of practical size, consisting of one ^{15}N and six methyl ^{1}H spins, with $J_m = 0.82$ Hz. The ^{1}H resonance frequency was set to 500 MHz and the carrier frequencies were set on resonance with the ^{15}N and methyl ^{1}H spins. The REBURP and the nonselective pulses were simulated with finite widths corresponding to the experimental

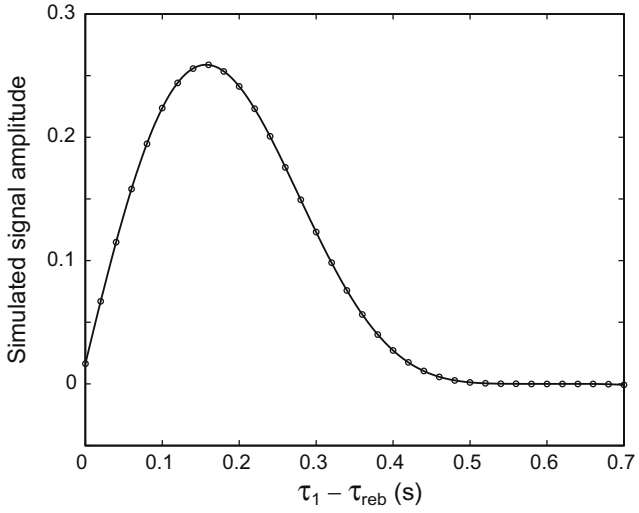

Fig. 4. Numerical simulation of the selective ^{15}N-to-^{1}H INEPT pulse sequence acting on a simplified spin system. Circles are simulated methyl ^{1}H signal amplitudes for different values of the INEPT transfer delay ($\tau_1 - \tau_{reb}$). The line was calculated using a modified form of Eq. (1) with parameter values from a least-squares fit to the data. This fit was used to determine τ_{reb}, the effective evolution time of the ^{15}N–methyl ^{1}H coupling during the sequence's REBURP pulse.

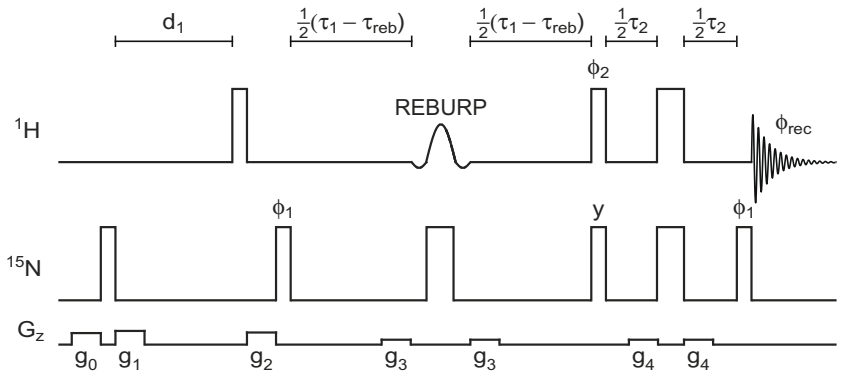

Fig. 3. Selective refocused INEPT pulse sequence for coherent polarization transfer from ^{15}N to methyl ^{1}H in ^{15}N-choline. Narrow (wide) rectangles denote radiofrequency pulses with a tip angle of $\pi/2$ (π), applied with B_1 field strengths of 23.9 kHz for ^{1}H and 15.6 kHz for ^{15}N. The shaped ^{1}H pulse is a 6.695 ms REBURP [12] centered on the methyl ^{1}H frequency. A four step phase cycle ($\phi_1 = x, x, x, x$; $\phi_2 = x, y, x, y$; $\phi_{rec} = x, y, x, y$) was used to suppress signals originating from ^{1}H magnetization and to prevent carry over of signal from one transient to the next. A recycle delay d_1 of 60 s ($\sim$0.25 T_1) was used. Since it is impractical to make this delay long enough to allow full relaxation of the choline ^{15}N spin, a purge element consisting of a ^{15}N $\pi/2$ pulse sandwiched by gradients g_0 and g_1 is used to eliminate ^{15}N magnetization at the start of d_1, ensuring a consistent starting magnetization for all experiments. A ^{1}H purge element comprising a ^{1}H $\pi/2$ pulse and gradient g_2 is used at the start of each transient. Gradients g_3 and g_4 are used to suppress coherence transfer pathways created by imperfect π pulses.

values. Relaxation and phase cycling were neglected. The pulse sequence shown in Fig. 3 was simulated, and the methyl ^{1}H signal amplitude was calculated, for each of a series of values of the INEPT transfer delay ($\tau_1 - \tau_{reb}$). The signal data, shown in Fig. 4, was then subjected to least-squares fit to a version of Eq. (1) appropriate for a system containing six methyl ^{1}H spins and including τ_{reb} as an adjustable parameter, resulting in the value of τ_{reb} = 6.4 ms used experimentally.

4. Results and discussion

Fig. 5 shows a spectrum of ^{15}N-choline recorded using the selective ^{15}N-to-^{1}H INEPT sequence of Fig. 3, alongside a ^{15}N-detected spectrum of the same sample recorded in a similar measurement time. It is not meaningful to compare these spectra quantitatively because they were both recorded using a probe that is optimized for direct heteronuclear observation, a factor which diminishes the sensitivity advantage of ^{1}H detection. However, even under these unfavorable circumstances the sensitivity to ^{15}N magnetization is more than an order of magnitude better in the selective INEPT spectrum (Fig. 5a) than in the ^{15}N-detected spectrum (Fig. 5b).

A modified version of the selective ^{15}N-to-^{1}H INEPT experiment was used to measure the ^{15}N longitudinal relaxation time of ^{15}N-choline in D_2O solution, yielding a value of $T_1 = (217 \pm 38)$ s (Fig. 6). This is comparable to the value $T_1 = (285 \pm 12)$ s previously reported by Gabellieri et al. [3] for ^{15}N-choline in 90% H_2O/10% D_2O.

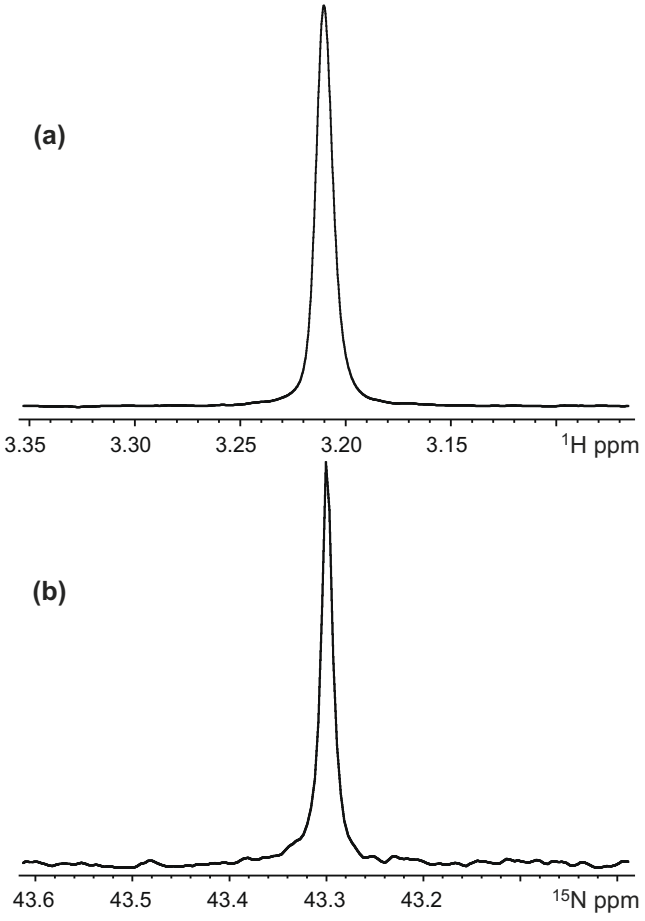

Fig. 5. (a) ^{1}H spectrum of ^{15}N-choline recorded using the selective ^{15}N-to-^{1}H INEPT sequence of Fig. 3. Only the methyl resonance is shown. (b) Single-pulse ^{15}N spectrum of ^{15}N-choline, recorded with tip angle $\pi/2$. Spectra (a) and (b) were each collected on the same Varian AutoX Dual Broadband probe, taking the sum of four transients with a recycle delay of 60 s. Monte Carlo fits of (a) and (b) to Lorentzian lineshapes show that, relative to direct ^{15}N detection, the fractional uncertainty in the initial ^{15}N magnetization is reduced by a factor of 11.0 when using the selective ^{15}N-to-^{1}H INEPT sequence, even though the probe design is optimized for the ^{15}N channel.

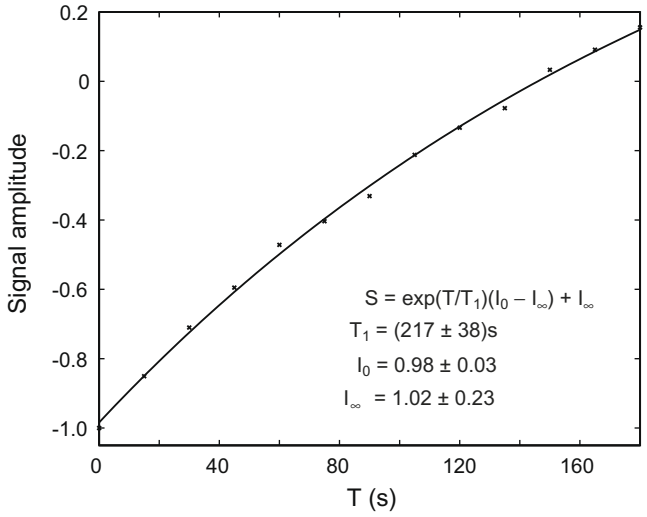

Fig. 6. Measurement of the ^{15}N longitudinal relaxation time of ^{15}N-choline in D_2O solution using a modified version of the pulse sequence shown in Fig. 3. The experiment was repeated for 13 values of the inversion-recovery delay T = 0.001, 15, 30, 45, ..., 180 s. Crosses are experimental methyl ^{1}H signal amplitudes obtained by integrating the spectral data. The line was calculated using the indicated equation and parameter values from a least-squares fit to the data.

A series of ^{15}N-choline ^{15}N-to-^{1}H INEPT spectra were recorded using both selective and nonselective versions of the pulse sequence of Fig. 3 with values of the transfer delay τ_1 ranging from 6.4 ms to 700 ms. The methyl ^{1}H signal amplitudes observed in these experiments are plotted in Fig. 7. The selective INEPT sequence allows ^{15}N-choline to be detected with 52% greater sensitivity than the nonselective sequence, comparing the maximum signal amplitude observed in each case. In the Theory section, the amplitude of the methyl ^{1}H signal was predicted as a function of the transfer delay for the selective (Eq. (1)) and nonselective (Eq. (2)) experiments using a product operator analysis. By fitting the

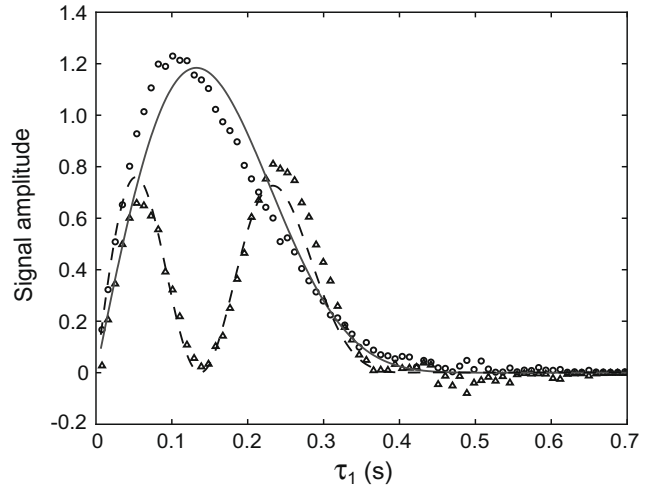

Fig. 7. Amplitude of the methyl ^{1}H signal observed in ^{15}N-to-^{1}H INEPT spectra of ^{15}N-choline using selective (circles) and nonselective (triangles) versions of the pulse sequence shown in Fig. 3, as a function of the INEPT transfer period τ_1. The lines were calculated using Eq. (1) (solid line) and Eq. (2) (dashed line) with parameter values from a least-squares fit to the data.

observed signal amplitudes to Eqs. (1) and (2), the optimal length of τ_1 for each experiment can be determined, as well as precise values of choline's ^{15}N–^{1}H coupling constants.

A simultaneous least-squares fit to both datasets yields parameter values $A_{sel} = 0.632 \pm 0.001$, $A_{non} = 1.000 \pm 0.005$, $J_m = (0.817 \pm 0.001)$ Hz, $J_b = (3.64 \pm 0.01)$ Hz, and $C = 0.000 \pm 0.001$. These values for the coupling constants are similar to ones derived from previously published ^{1}H–^{14}N values ($J_m = 0.80$ Hz and $J_b = 3.61$ Hz) [15] or observed recently [6] with ^{15}N-choline ($J_m = 0.8$ Hz and $J_b = 3.7$ Hz). The value of the smaller ^{15}N–methylene ^{1}H coupling constant was found to have a negligible effect on the fitting process, so this parameter was fixed at a reasonable value of $J_a = -0.57$ Hz.

Note that, for experiments using the selective and nonselective versions of the pulse sequence of Fig. 3 on the same spectrometer hardware and sample, the constants in Eqs. (1) and (2) should ideally be the same. The observation that A_{sel} is smaller than A_{non} may be due to signal losses during the selective sequence's REBURP pulse. Comparing the values of A_{sel} and A_{non} from the least-squares fit it appears that 36% of the signal is lost in this way. This can be attributed in part to miscalibration of the REBURP pulse. A three pulse sequence ($\pi/2 - \text{REBURP} - \pi/2$) was used to calibrate the REBURP pulse by seeking pulse width and power parameters that gave the best null signal. It would be more appropriate to choose a calibration sequence that uses the REBURP pulse for inversion, as it is used in the selective INEPT sequence, rather than for refocusing. Another possibility for the relative deviations of the selective and nonselective experiments from the theory is that ^{1}H–^{1}H couplings are neglected in the analytical theory given for the dynamics. Including these numerically is beyond our present computer capabilities.

We have presented a pulse sequence that suppresses the effects of the four methylene protons on the INEPT transfer from ^{15}N to methyl ^{1}H in ^{15}N-choline. Note that the same result can be achieved by selective deuteration of ^{15}N-choline. This approach might provide the additional benefit of increasing the molecule's ^{15}N longitudinal relaxation time and would be an option for DNP experiments. However, the present selective recoupling strategy is clearly advantageous for ^{15}N-choline hyperpolarization using PASADENA. In these experiments, two of the methylene ^{1}H spins derive from a parahydrogen molecule which reacts with an unsaturated precursor to initiate the hyperpolarization process. Although deuteration of the alkene precursor can remove two of the methylene ^{1}H spins, those which supply the spin order cannot be eliminated.

The success of this selective coherence transfer strategy in ^{15}N-choline has clear implications for studies of other hyperpolarized small biomolecules. By directing the spin order to a subset of the possible detection spins, sensitivity is improved. The recoupling strategy demonstrated here accomplishes this by way of a frequency selective π pulse, which simplifies, and often shortens, the polarization transfer step. Similar selective INEPT sequences could be used to improve the sensitivity of the ^{13}C-to-^{1}H polarization transfer experiments demonstrated by Chekmenev et al. in hyperpolarized TFPP [4] by directing the spin order to one of the resolved ^{1}H sites.

The selective ^{15}N-choline transfer presented here also has potentially useful applications to thermally polarized *in vivo* ^{15}N spectroscopy. Pulse sequences can be devised to transfer methyl ^{1}H polarization to ^{15}N for an encoding period and then back to methyl ^{1}H for detection. Such sequences would benefit from choline's long ^{15}N T_1 while making use of the strong thermal polarization of the nine methyl ^{1}H spins. This strategy is equally applicable if the ^{15}N polarization is selectively recoupled to the methylene protons adjacent to the oxygen, which more readily resolve choline from acetylcholine and phospholine [6]. To lengthen the time available for the metabolic interconversion of choline and related compounds, chemical exchange is best encoded in the difference between longitudinal ^{15}N magnetization of the various species, prior to selective polarization transfer.

5. Conclusion

As part of a strategy to improve the sensivity of *in vivo* experiments on hyperpolarized small biomolecules, we have investigated INEPT pulse sequences for the transfer of magnetization from ^{15}N to the methyl ^{1}H spins in ^{15}N-choline. Product operator analysis of a simple refocused INEPT sequence shows that the optimized efficiency of this transfer is diminished by 62% by the action of competing couplings between ^{15}N and choline's methylene ^{1}H spins. A selective INEPT sequence, using a ^{1}H REBURP pulse to suppress undesired couplings during the transfer period, was devised and tested *in vitro* on a thermally polarized ^{15}N-choline sample. It was demonstrated that the selective INEPT sequence leads to a 52% stronger methyl ^{1}H signal than the nonselective version.

Acknowledgments

This work was supported by the Beckman Institute pilot program, "Spin-Polarized Molecules for Structural and Systems Biology". JEO was supported by a Postdoctoral Fellowship from the Natural Sciences and Engineering Research Council of Canada.

References

[1] E.Y. Chekmenev, J. Hovener, V.A. Norton, K. Harris, L.S. Batchelder, P. Bhattacharya, B.D. Ross, D.P. Weitekamp, PASADENA hyperpolarization of succinic acid for MRI and NMR spectroscopy, J. Am. Chem. Soc. 130 (2008) 4212–4213.
[2] K. Golman, R.I. Zandt, M. Lerche, R. Pehrson, J.H. Ardenkjaer-Larsen, Metabolic imaging by hyperpolarized ^{13}C magnetic resonance imaging for in vivo tumor diagnosis, Cancer Res. 66 (2006) 10855–10860.
[3] C. Gabellieri, S. Reynolds, A. Lavie, G.S. Payne, M.O. Leach, T.R. Eykyn, Therapeutic target metabolism observed using hyperpolarized ^{15}N choline, J. Am. Chem. Soc. 130 (2008) 4598–4599.
[4] E.Y. Chekmenev, V.A. Norton, D.P. Weitekamp, P. Bhattacharya, Hyperpolarized ^{1}H NMR employing low γ nucleus for spin polarization storage, J. Am. Chem. Soc. 131 (2009) 3164–3165.
[5] G.A. Morris, R. Freeman, Enhancement of nuclear magnetic resonance signals by polarization transfer, J. Am. Chem. Soc. 101 (1979) 760–762.
[6] R. Sarkar, A. Comment, P.R. Vasos, S. Jannin, R. Gruetter, G. Bodenhausen, H. Hall, D. Kirik, V.P. Denisov, Proton NMR of ^{15}N-choline metabolites enhanced by dynamic nuclear polarization, J. Am. Chem. Soc. 131 (2009) 16014–16015.
[7] J.A. Pfeilsticker, J.E. Ollerenshaw, V.A. Norton, D.P. Weitekamp, Reverse ^{15}N rINEPT with selective recoupling in choline, in: 50th Experimental NMR Conference, Asilomar, 2009.
[8] Y. Boulanger, M. Labelle, A. Khiat, Role of phospholipase A_2 on the variations of the choline signal intensity observed by ^{1}H magnetic resonance spectroscopy in brain diseases, Brain Res. Rev. 33 (2000) 380–389.
[9] R. Katz-Brull, D. Seger, D. Rivenson-Segal, E. Rushkin, H. Degani, Metabolic markers of breast cancer: enhanced choline metabolism and reduced choline–ether–phospholipid synthesis, Cancer Res. 62 (2002) 1966–1970.
[10] E. Sutinen, M. Nurmi, A. Roivainen, M. Varpula, T. Tolvanen, P. Lehikoinen, H. Minn, Kinetics of [^{11}C]choline uptake in prostate cancer: a PET study, Eur. J. Nucl. Med. Mol. Imaging 31 (2004) 317–324.
[11] D.M. Doddrell, D.T. Pegg, W. Brooks, M.R. Bendall, Enhancement of ^{29}Si or ^{119}Sn NMR signals in the compounds $M(CH_3)_nCl_{4-n}$ (M = Si or Sn, $R = 4, 3, 2$) using proton polarization transfer. Dependence of the enhancement on the number of scalar coupled protons, J. Am. Chem. Soc. 103 (1981) 727–728.
[12] H. Geen, R. Freeman, Band-selective radiofrequency pulses, J. Magn. Reson. 93 (1991) 93–141.
[13] W.H. Press, S.A. Teukolsky, W.T. Vetterling, B.P. Flannery, Numerical Recipes in C: The Art of Scientific Computing, second ed., Cambridge University Press, Cambridge, UK, 1992.
[14] S.A. Smith, T.O. Levante, B.H. Meier, R.R. Ernst, Computer simulations in magnetic resonance. An object-oriented programming approach., J Magn. Reson. A106 (1994) 75–105.
[15] V. Govindaraju, K. Young, A.A. Maudsley, Proton NMR chemical shifts and coupling constants for brain metabolites, NMR in Biomedicine 13 (2000).